Evaluation of Prostate Cancer with PET/MRI

Liza Lindenberg[1], Mark Ahlman[2], Baris Turkbey[1], Esther Mena[3], and Peter Choyke[1]

[1]Molecular Imaging Program, Center for Cancer Research, National Cancer Institute, National Institutes of Health, Bethesda, Maryland; [2]Department of Radiology and Imaging Sciences, National Institutes of Health Clinical Center, Bethesda, Maryland; and [3]Russell H. Morgan Department of Radiology and Radiological Science, Johns Hopkins Medical Institutions, Baltimore, Maryland

In the ongoing effort to understand and cure prostate cancer, imaging modalities are constantly evolving to assist in clinical decisions. Multiparametric MRI can be used to direct prostate biopsies, improve diagnostic yield, and help clinicians make more accurate decisions. PET is superior in providing biologic information about the cancer and is sensitive and highly specific. Integrated PET/MRI is a welcome technical advance with great potential to influence the diagnosis and management of prostate cancer in clinical practice.

Key Words: multiparametric MRI; PET/MRI; prostate cancer

J Nucl Med 2016; 57:111S–116S
DOI: 10.2967/jnumed.115.169763

Prostate cancer (PCa) is the second leading cause of cancer mortality in men in the United States. Because PCa tumors usually grow slowly, many men live with this cancer (>2.9 million men in the United States); this situation represents a large burden of disease (*1*). Given the sizable number of affected individuals, imaging methods for improving diagnosis, assessing the response to therapy, and identifying early recurrence are of great interest. Imaging modalities that have traditionally been used to assess PCa include transrectal ultrasound (TRUS), CT, MRI, and nuclear bone scanning. MRI, in particular, has had a major impact on the diagnosis of PCa. It can be used to localize and guide the biopsy of focal lesions, thus supplementing traditional "blind" biopsies of the prostate. In recent years, considerable progress has been made with PET/CT, along with novel PCa-targeted agents. Combining the virtues of prostate MRI with PET is now possible with the development of new PET/MRI hybrid cameras; this technique holds unique promise for evaluating PCa. Here, we review the benefits of separate PET and MRI for PCa and then explore the potential value of integrating them into a single PET/MRI examination.

MRI AND PROSTATE CANCER

Multiparametric MRI (mpMRI), which includes both anatomic (T2-weighted MRI) and functional (diffusion-weighted MRI and dynamic contrast–enhanced MRI) pulse sequences, has been an integral component of PCa management for the last decade. More commonly used for mapping localized PCa, it has been beneficial in guiding biopsies, even in patients with persistently high serum prostate-specific antigen (PSA) levels and inconclusive workups, as well as for treatment follow-up in patients after definitive therapy (*2*). However, the staging of PCa has been more challenging.

The current standard approach to primary PCa diagnosis is based on random TRUS-guided biopsies. This approach has been criticized because it often yields an overdiagnosis of indolent disease and an underdiagnosis of clinically significant cancer (*3,4*). mpMRI can be used to assist prostate biopsies through image guidance. This procedure can be done directly in the bore of the MRI scanner (in-gantry biopsy) or in the ultrasound suite (MRI–TRUS fusion or "cognitive" fusion biopsy). Regardless of the method used, mpMRI guidance has been reported to result in increased diagnostic yield for clinically significant cancers and, thus, improved patient care (*5–8*). Nevertheless, the widespread use of mpMRI has been hindered by its relatively high cost, its complexity, and lack of training (*9*).

In the staging of localized PCa, the results of using mpMRI to identify extraprostatic extension (EPE) and seminal vesicle invasion (SVI) have been promising (*10*). For the assessment of EPE with mpMRI, the sensitivity ranged from 50% to 86% and the specificity was approximately 95% (*10,11*). However, the current consensus is that mpMRI is more specific for ruling out EPE than it is sensitive for visualizing EPE (*12*). Gross extension of tumor beyond the prostate capsule is highly reliable, but more subtle extension can be due to EPE or inflammatory or traumatic changes induced by biopsy. Attempts to overcome this challenge include assessing tumor contact length; however, this technique is still considered exploratory, and further evaluation in larger studies is needed (*13*). The detection of SVI with mpMRI has followed a similar trajectory. In a cohort of 376 patients, the sensitivity and the specificity for SVI were 49% and 98%, respectively (*14*). In a study of 822 patients, 31 had suspected SVI on mpMRI; in this population, the rate of detection with MRI-targeted biopsy was 65% (*15*). Therefore, mpMRI has limitations in sensitivity but yields few false-positive findings and therefore has high specificity. Naturally, because interpretation is subjective, strict criteria for assessing EPE and SVI must be used. mpMRI currently is the most encouraging pretreatment method for staging, but there is room for improvement.

Recent studies have suggested that mpMRI can also be used in the evaluation of recurrent or residual disease (*16–18*). Most recurrences occur in the prostatectomy bed (after surgery) or within the prostate (after radiotherapy). However, treatment-induced changes, including distorted anatomy, fibrosis, artifacts from surgical clips, and alteration of the signal characteristics on mpMRI, can complicate the interpretation and hinder the ability of mpMRI to diagnose

Received Mar. 3, 2016; revision accepted May 24, 2016.
For correspondence or reprints contact: Liza Lindenberg, Molecular Imaging Program, Center for Cancer Research, National Cancer Institute, National Institutes of Health, Bldg. 10, Room B3B402 MS 1088, 10 Center Dr., Bethesda, MD 20892.
E-mail: liza.lindenberg@mail.nih.gov

lesions. Suggestive findings still need to be confirmed by histopathology. Although experience remains limited, early results with mpMRI in the setting of biochemical recurrence suggest that it can be sensitive but lacks specificity (*17*).

MRI appears to be useful in the early detection of bone metastases. Normal bone marrow has a homogeneous signal intensity, depending on the pulse sequence. Early metastatic disease creates a heterogeneous signal within the marrow space, making MRI very sensitive for bone metastases. In a recent study of PCa-related bone disease in 8 patients who underwent ^{68}Ga-labeled prostate-specific membrane antigen (PSMA) PET/MRI, all 28 metastatic bone foci were seen on MRI, which performed as well as ^{68}Ga-PSMA PET and better than low-dose CT (*19*). Recently, the diagnostic accuracy of whole-body MRI coupled with diffusion-weighted (DW) imaging has been promising, with a reported sensitivity of 91%; the sensitivity for ^{18}F-NaF PET/CT was 93%. MRI also had fewer equivocal findings than nuclear bone scanning and PET (*20*). Whole-body MRI, including DW MRI, has the potential to augment nuclear bone scanning or ^{18}F-NaF PET/CT; however, further research is needed to validate these early reports.

Therefore, the primary role of mpMRI is to identify focal lesions within the prostate for targeted biopsy. For staging of the prostate capsule and the seminal vesicles, mpMRI has a very high specificity, mainly because of the large number of true-negative studies. It has variable sensitivity for EPE and SVI. More recently, mpMRI has been used to detect recurrent disease after radiation therapy or surgery, but the findings are nonspecific and typically require biopsy for confirmation.

PET AND PROSTATE CANCER

Several studies have investigated the potential utility of PET/CT imaging with different radiotracers for PCa, including ^{18}F-FDG, ^{11}C-acetate, ^{11}C- or ^{18}F-choline, anti–1-amino-3-^{18}F-fluorocyclobutane-1-carboxylic acid, 16α-^{18}F-fluoro-5α-dihydrotestosterone and, more recently, radiolabeled PSMA ligands and gastrin-releasing peptide receptors (*21*). Table 1 summarizes the main PET tracers available or under development. These agents are reviewed in more detail in this special issue and are not discussed in depth in this article.

A general limitation of PET imaging in assessing primary PCa is that the spatial resolution limits the reliability for the detection of small lesions; however, in the presence of abundant overexpression of the target, very small lesions may be visualized by PET. Many radiotracers also show nonspecific uptake at sites of benign prostatic hyperplasia (*22*). To date, no PET-based imaging modalities have shown any benefit over MRI in the imaging of early PCa. More favorable data for PET imaging have been reported for the staging of high-risk PCa and biochemical relapse after definitive therapy.

^{11}C- or ^{18}F-choline, a marker of cell membrane metabolism, has been used worldwide in the setting of suspected biochemical relapse, and its uptake correlates with serum PSA levels and doubling time (*23,24*). The diagnostic performance of radiolabeled choline PET/CT imaging in detecting bone metastases was compared with those of MRI, bone SPECT, and planar bone scintigraphy in a metaanalysis; the pooled sensitivities for ^{11}C- or ^{18}F-choline PET/CT, MRI, and planar bone scintigraphy were 99%, 95%, and 82%, respectively (*25*). Skeletal metastatic disease was also assessed with high sensitivity by ^{18}F-NaF (*26*).

The latest PET molecular imaging agents have been developed to target PSMA (*27*). Recent data suggested that ^{68}Ga-PSMA may be more sensitive than ^{11}C- or ^{18}F-choline PET/CT in patients with biochemical failure and low PSA levels (*28*).

The first ^{18}F-labeled PSMA ligand, *N*-[*N*-[(*S*)-1,3-dicarboxypropyl]-carbamoyl]-4-^{18}F-fluorobenzyl-L-cysteine (^{18}F-DCFBC), appears to show superiority in the detection of early bone metastases (*29*) but is limited for the assessment of primary PCa. ^{18}F-DCFBC PET localized high-grade tumors and most clinically significant tumor lesions but was limited in the detection of smaller tumors (<1.1 mL) and lower-grade tumors (Gleason score of 7 or 6) (*30*). In addition, persistent background vascular activity was a challenge in the interpretation of images. A second-generation ^{18}F-labeled PSMA ligand, 2-(3-(1-carboxy-5-[(6-^{18}F-fluoro-pyridine-3-carbonyl)-amino]-pentyl)-ureido)-pentanedioic acid (*31*), had an affinity 5 times higher than that of ^{18}F-DCFBC.

The strengths of PET/CT for PCa are its abilities to image the whole body in one session and to survey for distant disease. Bone, lung, and outlying lymph nodes can be easily assessed for suspected tracer activity. Although CT can identify nodes that show uptake, the localization of lesions within and around the prostate or prostate bed may be challenging because the tissue contrast of CT in the pelvis is limited. Distinguishing the prostate gland and seminal vesicles from muscles, ligaments, and the bladder or rectal wall with CT can be difficult. Conversely, the excellent contrast resolution of MRI in the prostate allows many different structures, such as the peripheral zone, transition zone, urethra, prostate capsule, and seminal vesicles, to be readily identified. In bone, CT is quite good at detecting osteoblastic lesions for correlation with PET findings; however, CT findings often are negative at a site at which PET findings are positive, raising questions about false-positive findings. In this setting, MRI may be more sensitive for detecting subtle alterations in bone structure that are indicative of early metastases.

A consideration with PET/CT is ionizing radiation exposure. The CT component of a PET/CT scan contributes approximately 73% of the total effective dose unless modern low-dose CT techniques are used (*32*). However, efforts to decrease CT radiation exposure come at the expense of decreased image quality and anatomic detail. Therefore, in many respects, a more ideal pairing of modalities is PET and MRI, especially in the pelvis.

PET/MRI

The case for PET/MRI centers on the comparative strengths of both modalities. MRI is superior in diagnosing and characterizing localized soft-tissue disease and assisting in the evaluation of specific bone lesions, especially with T1-weighted and DW imaging. PET is superior in providing biologic information about the cancer and is sensitive and highly specific for residual or recurrent disease. Combining the 2 systems is appealing but technically challenging. Hybrid PET/MRI machines were first clinically introduced in 2010. Initial experience showed the feasibility of PET/MRI and comparability to PET/CT in oncology (*33*). In combined systems, the PET machinery must accommodate the strong magnetic field of MRI; therefore, avalanche photodiodes or new semiconductor detectors, such as solid-state silicon photomultipliers, are used. Several vendors have since introduced PET/MRI units that can produce simultaneous and superimposed imaging.

The first simultaneous PET/MRI unit to achieve U.S. Food and Drug Administration approval for clinical use was the Biograph mMR (Siemens). The unit uses an array of avalanche photodiodes to detect coincident photon emissions within a 3-T field strength. The Signa PET/MRI unit was recently produced by General Electric

TABLE 1
Potential PET Tracers for Prostate Cancer

PET tracer	Mechanism
^{18}F-FDG	Glucose metabolism
^{11}C- or ^{18}F-acetate	Lipid metabolism
^{11}C- or ^{18}F-choline	Lipid metabolism
^{11}C-methionine	Amino acid transport
^{18}F-FACBC	Amino acid transport
^{18}F-DCFBC, ^{18}F-DCFPyL, ^{64}Cu- or ^{89}Zr-J591, and ^{68}Ga-PSMA compounds: ^{68}Ga-DKFZ-PSMA-1 (same as ^{68}Ga-PSMA-HBED-CC), ^{68}Ga-PSMA-DKFZ-617, and ^{68}Ga-PSMA I&T	PSMA inhibitors/antibodies
^{18}F-FDHT	Androgen receptor
^{18}F-FLT	Cell proliferation
^{18}F-FMAU	Cell proliferation
^{18}F-NaF	Calcium analog
^{68}Ga-bombesin	Gastrin-releasing peptide receptor

^{18}F-FACBC = 1-amino-3-^{18}F-fluorocyclobutane-1-carboxylic acid; ^{18}F-DCFPyL = 2-(3-(1-carboxy-5-[(6-^{18}F-fluoro-pyridine-3-carbonyl)-amino]-pentyl)-ureido)-pentanedioic acid; DKFZ = Deutsches Krebsforschungszentrum (German Cancer Research Center); I&T = imaging and therapy; ^{18}F-FDHT = 16α-^{18}F-fluoro-5α-dihydrotestosterone; ^{18}F-FLT = 3′-deoxy-3′-^{18}F-fluorothymidine; ^{18}F-FMAU = 1-(2′-deoxy-2′-^{18}F-fluoro-β-D-arabinofuranosyl)thymine.

and approved for clinical use. This unit applies silicon-based photomultiplier tubes that afford fine temporal discrimination of photon detection events to allow for time-of-flight PET image reconstruction. Naturally, because these units combine two costly modalities into one, they are expensive, with each creating difficult engineering challenges for the other. One limitation of current simultaneous PET/MRI units lies in the availability of an MRI field strength of only 3 T. Indeed, certain advantages exist for 1.5-T MRI, including improved magnetic field homogeneity, which reduces certain artifacts. Nonetheless, successful PET/MRI scanning is now possible at many academic centers (Fig. 1).

Regarding the implementation of PET/MRI in a clinical setting, several considerations exist. In our experience, conducting a PET/MRI examination requires high levels of skill and experience on the part of the technologist, for several reasons. A busy MRI department requires flexibility in a shifting environment. Often, certain MR sequences must be repeated at the time of the examination because of issues, common to MRI (e.g., motion and artifacts), that lead to poor image quality; this situation can result in significant delays. These concerns happen in a setting in which the time between the uptake of a PET radiopharmaceutical injection and imaging must be rigorously standardized. Moreover, to avoid accidents, PET technologists must be cognizant of the safety issues encountered during work in a high-magnetic-field environment.

PET/MRI interpretation also requires varied approaches. The detection of bone and lung lesions on MRI appears to be most affected by the integrated scanner. Much has been published about various methods for MRI-based attenuation correction. The first step in creating MR attenuation correction maps involves the segmentation of in- and out-of-phase images, which are then used to infer the location and attenuation coefficients of water, fat, lung, and air (*34*). One issue is the inability of these images to accurately map bone; this issue is important in PCa because of its frequent metastases to this system. Special attenuation correction based on MR sequences usually results in a quantitative underestimation of SUVs in bone. Errors in SUVs of bone lesions can range from 15% to 20% (*35*). However, in our experience, these errors do not significantly affect the visual conspicuity of lesions on PET/MRI if uptake is sufficient to be perceptible on PET/CT. Indeed, some have suggested that the combination of PET and MRI increases the diagnostic confidence of prostate bone metastases over that of PET/CT (*36*). Furthermore, regardless of the radiopharmaceutical used, this systematic bias for the underestimation of SUVs is expected to

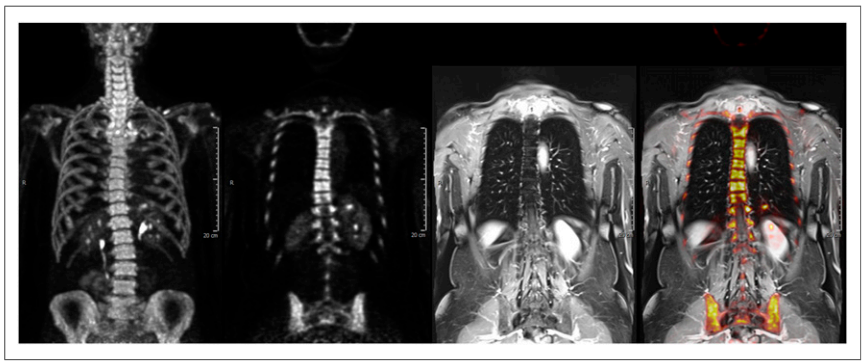

FIGURE 1. Normal coronal ^{18}F-NaF PET/MR images representing (from left to right) PET maximum-intensity projection, PET coronal slice, T1-weighted MR image, and fusion of PET with MRI.

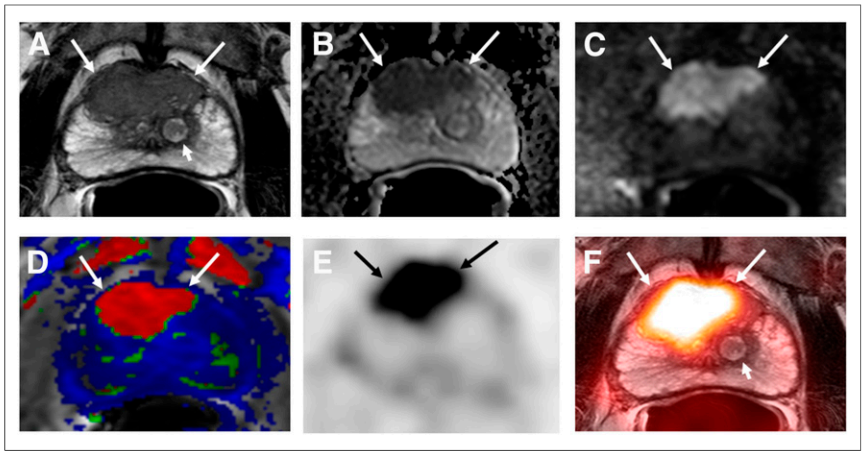

FIGURE 2. 73-y-old man (serum PSA, 38 ng/mL) with history of 2 negative TRUS-guided prostate biopsies. (A) Axial T2-weighted MRI shows hypointense lesion in midline anterior transition zone (A) (long arrows); short arrow indicates benign hyperplastic lesion. (B and C) Lesion had restricted diffusion on apparent-diffusion-coefficient maps (B) and DW MRI (b = 2,000 s/mm^2) (C) (arrows). (D) On permeability map derived from dynamic contrast-enhanced MRI, lesion—in comparison with remainder of prostate—has increased vascularity (arrows). (E and F) ^{18}F-DCFBC PET (E) and software-based PET/MRI fusion (F) images show specific uptake within midline anterior transition zone lesion (long arrows); benign hyperplastic nodule in left transition zone did not show any ^{18}F-DCFBC uptake (short arrow). TRUS/MRI fusion–guided biopsy of this lesion revealed prostate adenocarcinoma with Gleason scores of 4 and 5.

be present on each examination longitudinally, thus still allowing for accurate estimation of changes in SUV over time.

PET/MRI IN LOCALIZED AND BIOCHEMICALLY RECURRENT DISEASE

Spick et al. conducted an excellent literature review comparing PET/MRI with PET/CT in about 2,300 oncology patients and found similar performance levels overall (*37*). Specific reports evaluating PET/MRI for PCa are few. PET/CT and PET/MRI were studied with ^{11}C-choline in 32 men with primary or biochemically recurrent PCa (*38*). Lesion detection was comparable for both, but PET/MRI was better at the anatomic allocation of lesions, especially in the bone and pelvis. Wetter et al. evaluated the 2 systems with ^{18}F-choline in a mixed group of patients with primary PCa and patients who had undergone prostatectomy and had rising PSA levels (*39*). PET/MRI and PET/CT detected the same lesions, but quantitative parameters were significantly lower with PET/MRI, likely because of the use of different attenuation correction methods (*39*).

The first published report of the use of ^{68}Ga-PSMA-HBED-CC (^{68}Ga-PSMA—a radioconjugate composed of a prostate-specific membrane antigen [PSMA]–targeting ligand, Glu-urea-Lys(Ahx)[Glu-NH-CO-NH-Lys(Ahx)], conjugated to ^{68}Ga via the acyclic radiometal chelator *N,N′*-bis[2-hydroxy-5-(carboxyethyl)benzyl]ethylenediamine-*N,N′*-diacetic acid [HBED-CC]) with PET/MRI showed that this method was slightly better at characterizing PCa lesions than PET/CT (*40*). In 20 men with biochemical recurrence, some mismatch in lesion detection and dropout of tracer activity attributed to scatter correction were noted on several PET/MR images. A recently published article reported a higher diagnostic accuracy of ^{68}Ga-PSMA-HBED-CC PET/MRI in localizing PCa than of either mpMRI or PET alone on the basis of sextant pathology; therefore, this technique could improve the diagnostic yield for needle biopsies in the future (*41*).

For evaluating the pelvis before and after prostatectomy, focal uptake from PET tracers can imply an increased likelihood of PCa in suggestive high-resolution images of the prostate, lymph nodes, and soft tissue obtained with mpMRI (Fig. 2). With its excellent soft-tissue contrast, MRI can overcome some of the limitations encountered with PET in evaluating anatomy because of intense physiologic radiotracer excretion through the bladder and urethra, especially in biochemically recurrent disease (Fig. 3) (*42*).

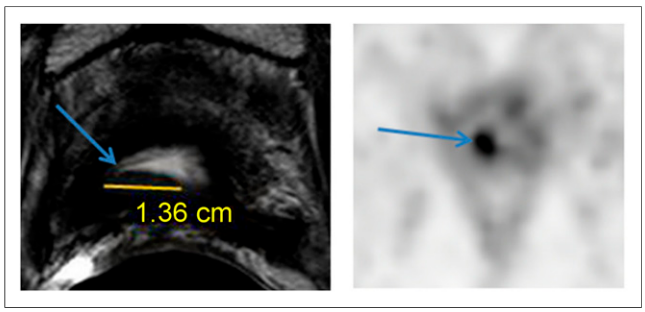

FIGURE 3. 64-y-old man with history of PCa treated by radical prostatectomy 4 y earlier and current biochemical recurrence (PSA, 0.61 ng/mL). Suggestive findings in prostate fossa on MRI (left) matched uptake on ^{18}F-DCFBC PET (right) (arrows).

PET/MRI IN METASTATIC DISEASE

The usefulness of PET/MRI for PCa lung lesions is still evolving. Lung nodules found in PCa patients were examined with ^{68}Ga-PSMA and PET/CT or PET/MRI to determine whether SUVs could differentiate the lesions or further classify the type of cancer (*43*). Quantitative measurements were unable to distinguish prostate lung metastases from primary lung tumor or tuberculosis. Possible explanations are flaws in tracer specificity or binding behavior. For PET/MRI, attenuation correction or lung segmentation could also have influenced the outcome (*44*). Without dedicated MR sequences specifically designed to characterize lung parenchyma, MRI generally has limited spatial resolution and more respiratory artifacts than CT (*45*).

The real impact of the new hybrid technology for PCa is improved accuracy in bone disease detection and characterization. Focal bone uptake with a tracer such as ^{18}F-NaF or radiolabeled PSMA or choline in PET is not always accompanied by characteristic osteoblastic features on CT, especially in the small space of a rib; consequently, the certainty of the malignant status of a lesion is decreased. MRI is more sensitive for the detection of bone metastases, especially when DW sequences are used (*46,47*). Hence, focal PET activity is complementary to morphologic MRI indices in the diagnosis of bone metastases.

PET/MRI still has some drawbacks to overcome; for example, there is a need to develop shorter but still sufficient acquisition

protocols and accurate bone segmentation for MR attenuation correction of whole-body sequences (*44,48*). Cost and availability are also significant issues. As with most new technologies not yet readily produced, the expense is high. The average cost for PET/MRI is $5–$7 million (U.S. dollars); in comparison, premium-grade PET/CT is typically half that amount or less. Currently, only 3 commercial manufacturers offer PET/MRI systems; only 2 of these systems are integrated units capable of simultaneous PET and MRI acquisitions.

CONCLUSION

Here, we briefly discussed the value of separate MRI and PET for PCa and reviewed early experience with the combined modalities. Despite limitations, most studies have found that the performance of PET/MRI is at least equivalent to, if not slightly better than, that of PET/CT (*37,49–51*). PET/MRI appears to add data not provided by PET/CT, and these data can significantly affect patient management (*42*). For PCa, integrated PET/MRI is a welcome technical advance with great potential to influence clinical practice by providing a more certain map of localized PCa to aid in targeted biopsies and therapy, to improve detection in biochemical recurrence, and to enhance the staging of metastatic disease. In many respects, PET/MRI is ideally suited for PCa because it combines the excellent anatomic and functional information of MRI with the higher specificity of PET, especially with the new generation of highly targeted PET agents for PCa. Increasing experience and improved MR attenuation correction maps and multiparametric sequences will provide more compelling support for the use of PET/MRI as a preferred imaging tool for PCa.

DISCLOSURE

No potential conflict of interest relevant to this article was reported.

REFERENCES

1. American Cancer Society. Cancer facts & figures 2016. http://www.cancer.org/research/cancerfactsstatistics/cancerfactsfigures2016/index. Accessed February 22, 2016.
2. Turkbey B, Brown AM, Sankineni S, Wood BJ, Pinto PA, Choyke PL. Multiparametric prostate magnetic resonance imaging in the evaluation of prostate cancer. *CA Cancer J Clin.* 2016;66:326–336.
3. Cooperberg MR, Broering JM, Kantoff PW, Carroll PR. Contemporary trends in low risk prostate cancer: risk assessment and treatment. *J Urol.* 2007;178(Suppl):S14–S19.
4. Cohen MS, Hanley RS, Kurteva T, et al. Comparing the Gleason prostate biopsy and Gleason prostatectomy grading system: the Lahey Clinic Medical Center experience and an international meta-analysis. *Eur Urol.* 2008;54:371–381.
5. Hoeks CM, Schouten MG, Bomers JG, et al. Three-tesla magnetic resonance-guided prostate biopsy in men with increased prostate-specific antigen and repeated, negative, random, systematic, transrectal ultrasound biopsies: detection of clinically significant prostate cancers. *Eur Urol.* 2012;62:902–909.
6. Puech P, Rouviere O, Renard-Penna R, et al. Prostate cancer diagnosis: multiparametric MR-targeted biopsy with cognitive and transrectal US-MR fusion guidance versus systematic biopsy—prospective multicenter study. *Radiology.* 2013;268:461–469.
7. Shakir NA, George AK, Siddiqui MM, et al. Identification of threshold prostate specific antigen levels to optimize the detection of clinically significant prostate cancer by magnetic resonance imaging/ultrasound fusion guided biopsy. *J Urol.* 2014;192:1642–1648.
8. Siddiqui MM, Rais-Bahrami S, Turkbey B, et al. Comparison of MR/ultrasound fusion-guided biopsy with ultrasound-guided biopsy for the diagnosis of prostate cancer. *JAMA.* 2015;313:390–397.
9. Fascelli M, Rais-Bahrami S, Sankineni S, et al. Combined biparametric prostate magnetic resonance imaging and prostate-specific antigen in the detection of prostate cancer: a validation study in a biopsy-naive patient population. *Urology.* 2016;88:125–134.
10. Cornud F, Flam T, Chauveinc L, et al. Extraprostatic spread of clinically localized prostate cancer: factors predictive of pT3 tumor and of positive endorectal MR imaging examination results. *Radiology.* 2002;224:203–210.
11. Bloch BN, Furman-Haran E, Helbich TH, et al. Prostate cancer: accurate determination of extracapsular extension with high-spatial-resolution dynamic contrast-enhanced and T2-weighted MR imaging—initial results. *Radiology.* 2007;245:176–185.
12. de Rooij M, Hamoen EH, Witjes JA, Barentsz JO, Rovers MM. Accuracy of magnetic resonance imaging for local staging of prostate cancer: a diagnostic meta-analysis. *Eur Urol.* 2016;70:233–245.
13. Baco E, Rud E, Vlatkovic L, et al. Predictive value of magnetic resonance imaging determined tumor contact length for extracapsular extension of prostate cancer. *J Urol.* 2015;193:466–472.
14. Roethke M, Kaufmann S, Kniess M, et al. Seminal vesicle invasion: accuracy and analysis of infiltration patterns with high-spatial resolution T2-weighted sequences on endorectal magnetic resonance imaging. *Urol Int.* 2014;92:294–299.
15. Raskolnikov D, George AK, Rais-Bahrami S, et al. Multiparametric magnetic resonance imaging and image-guided biopsy to detect seminal vesicle invasion by prostate cancer. *J Endourol.* 2014;28:1283–1289.
16. Abd-Alazeez M, Ramachandran N, Dikaios N, et al. Multiparametric MRI for detection of radiorecurrent prostate cancer: added value of apparent diffusion coefficient maps and dynamic contrast-enhanced images. *Prostate Cancer Prostatic Dis.* 2015;18:128–136.
17. Muller BG, Kaushal A, Sankineni S, et al. Multiparametric magnetic resonance imaging-transrectal ultrasound fusion-assisted biopsy for the diagnosis of local recurrence after radical prostatectomy. *Urol Oncol.* 2015;33:425.e1–425.e6.
18. Arrayeh E, Westphalen AC, Kurhanewicz J, et al. Does local recurrence of prostate cancer after radiation therapy occur at the site of primary tumor? Results of a longitudinal MRI and MRSI study. *Int J Radiat Oncol Biol Phys.* 2012;82:e787–e793.
19. Freitag MT, Radtke JP, Hadaschik BA, et al. Comparison of hybrid ^{68}Ga-PSMA PET/MRI and ^{68}Ga-PSMA PET/CT in the evaluation of lymph node and bone metastases of prostate cancer. *Eur J Nucl Med Mol Imaging.* 2016;43:70–83.
20. Jambor I, Kuisma A, Ramadan S, et al. Prospective evaluation of planar bone scintigraphy, SPECT, SPECT/CT, ^{18}F-NaF PET/CT and whole body 1.5T MRI, including DWI, for the detection of bone metastases in high risk breast and prostate cancer patients: SKELETA clinical trial. *Acta Oncol.* 2016;55:59–67.
21. Jadvar H. Positron emission tomography in prostate cancer: summary of systematic reviews and meta-analysis. *Tomography.* 2015;1:18–22.
22. Mena E, Turkbey B, Mani H, et al. ^{11}C-acetate PET/CT in localized prostate cancer: a study with MRI and histopathologic correlation. *J Nucl Med.* 2012;53:538–545.
23. Treglia G, Ceriani L, Sadeghi R, Giovacchini G, Giovanella L. Relationship between prostate-specific antigen kinetics and detection rate of radiolabelled choline PET/CT in restaging prostate cancer patients: a meta-analysis. *Clin Chem Lab Med.* 2014;52:725–733.
24. Giovacchini G, Picchio M, Scattoni V, et al. PSA doubling time for prediction of [^{11}C]choline PET/CT findings in prostate cancer patients with biochemical failure after radical prostatectomy. *Eur J Nucl Med Mol Imaging.* 2010;37:1106–1116.
25. Shen G, Deng H, Hu S, Jia Z. Comparison of choline-PET/CT, MRI, SPECT, and bone scintigraphy in the diagnosis of bone metastases in patients with prostate cancer: a meta-analysis. *Skeletal Radiol.* 2014;43:1503–1513.
26. Even-Sapir E, Metser U, Mishani E, Lievshitz G, Lerman H, Leibovitch I. The detection of bone metastases in patients with high-risk prostate cancer: ^{99m}Tc-MDP planar bone scintigraphy, single- and multi-field-of-view SPECT, ^{18}F-fluoride PET, and ^{18}F-fluoride PET/CT. *J Nucl Med.* 2006;47:287–297.
27. Osborne JR, Akhtar NH, Vallabhajosula S, Anand A, Deh K, Tagawa ST. Prostate-specific membrane antigen-based imaging. *Urol Oncol.* 2013;31:144–154.
28. Afshar-Oromieh A, Haberkorn U, Eder M, Eisenhut M, Zechmann CM. [^{68}Ga]gallium-labelled PSMA ligand as superior PET tracer for the diagnosis of prostate cancer: comparison with ^{18}F-FECH. *Eur J Nucl Med Mol Imaging.* 2012;39:1085–1086.
29. Rowe SP, Macura KJ, Ciarallo A, et al. Comparison of prostate-specific membrane antigen–based ^{18}F-DCFBC PET/CT to conventional imaging modalities for detection of hormone-naïve and castration-resistant metastatic prostate cancer. *J Nucl Med.* 2016;57:46–53.
30. Rowe SP, Gage KL, Faraj SF, et al. ^{18}F-DCFBC PET/CT for PSMA-based detection and characterization of primary prostate cancer. *J Nucl Med.* 2015;56:1003–1010.

31. Chen Y, Pullambhatla M, Foss CA, et al. 2-(3-{1-carboxy-5-[(6-[^{18}F]fluoro-pyridine-3-carbonyl)-amino]-pentyl}-ureido)-pentanedioic acid, [^{18}F]DCFPyL, a PSMA-based PET imaging agent for prostate cancer. *Clin Cancer Res.* 2011;17:7645–7653.
32. Schäfer JF, Gatidis S, Schmidt H, et al. Simultaneous whole-body PET/MR imaging in comparison to PET/CT in pediatric oncology: initial results. *Radiology.* 2014;273:220–231.
33. Drzezga A, Souvatzoglou M, Eiber M, et al. First clinical experience with integrated whole-body PET/MR: comparison to PET/CT in patients with oncologic diagnoses. *J Nucl Med.* 2012;53:845–855.
34. Berker Y, Franke J, Salomon A, et al. MRI-based attenuation correction for hybrid PET/MRI systems: a 4-class tissue segmentation technique using a combined ultrashort-echo-time/Dixon MRI sequence. *J Nucl Med.* 2012;53:796–804.
35. Samarin A, Burger C, Wollenweber SD, et al. PET/MR imaging of bone lesions: implications for PET quantification from imperfect attenuation correction. *Eur J Nucl Med Mol Imaging.* 2012;39:1154–1160.
36. Samarin A, Hullner M, Queiroz MA, et al. ^{18}F-FDG-PET/MR increases diagnostic confidence in detection of bone metastases compared with ^{18}F-FDG-PET/CT. *Nucl Med Commun.* 2015;36:1165–1173.
37. Spick C, Herrmann K, Czernin J. ^{18}F-FDG PET/CT and PET/MRI perform equally well in cancer: evidence from studies on more than 2,300 patients. *J Nucl Med.* 2016;57:420–430.
38. Souvatzoglou M, Eiber M, Takei T, et al. Comparison of integrated whole-body [^{11}C]choline PET/MR with PET/CT in patients with prostate cancer. *Eur J Nucl Med Mol Imaging.* 2013;40:1486–1499.
39. Wetter A, Lipponer C, Nensa F, et al. Evaluation of the PET component of simultaneous [^{18}F]choline PET/MRI in prostate cancer: comparison with [^{18}F]choline PET/CT. *Eur J Nucl Med Mol Imaging.* 2014;41:79–88.
40. Afshar-Oromieh A, Haberkorn U, Schlemmer HP, et al. Comparison of PET/CT and PET/MRI hybrid systems using a ^{68}Ga-labelled PSMA ligand for the diagnosis of recurrent prostate cancer: initial experience. *Eur J Nucl Med Mol Imaging.* 2014;41:887–897.
41. Eiber M, Weirich G, Holzapfel K, et al. Simultaneous Ga-PSMA HBED-CC PET/MRI improves the localization of primary prostate cancer. *Eur Urol.* January 18, 2016 [Epub ahead of print].
42. Catalano OA, Rosen BR, Sahani DV, et al. Clinical impact of PET/MR imaging in patients with cancer undergoing same-day PET/CT: initial experience in 134 patients—a hypothesis-generating exploratory study. *Radiology.* 2013;269:857–869.
43. Pyka T, Weirich G, Einspieler I, et al. ^{68}Ga-PSMA-HBED-CC PET for differential diagnosis of suggestive lung lesions in patients with prostate cancer. *J Nucl Med.* 2016;57:367–371.
44. Boellaard R, Quick HH. Current image acquisition options in PET/MR. *Semin Nucl Med.* 2015;45:192–200.
45. Rauscher I, Eiber M, Fürst S, et al. PET/MR imaging in the detection and characterization of pulmonary lesions: technical and diagnostic evaluation in comparison to PET/CT. *J Nucl Med.* 2014;55:724–729.
46. Hricak H, Choyke PL, Eberhardt SC, Leibel SA, Scardino PT. Imaging prostate cancer: a multidisciplinary perspective. *Radiology.* 2007;243:28–53.
47. Luboldt W, Kufer R, Blumstein N, et al. Prostate carcinoma: diffusion-weighted imaging as potential alternative to conventional MR and ^{11}C-choline PET/CT for detection of bone metastases. *Radiology.* 2008;249:1017–1025.
48. Bailey DL, Pichler BJ, Gückel B, et al. Combined PET/MRI: multi-modality multi-parametric imaging is here—summary report of the 4th International Workshop on PET/MR Imaging; February 23-27, 2015, Tübingen, Germany. *Mol Imaging Biol.* 2015;17:595–608.
49. Heusch P, Nensa F, Schaarschmidt B, et al. Diagnostic accuracy of whole-body PET/MRI and whole-body PET/CT for TNM staging in oncology. *Eur J Nucl Med Mol Imaging.* 2015;42:42–48.
50. Huellner MW, Appenzeller P, Kuhn FP, et al. Whole-body nonenhanced PET/MR versus PET/CT in the staging and restaging of cancers: preliminary observations. *Radiology.* 2014;273:859–869.
51. Al-Nabhani KZ, Syed R, Michopoulou S, et al. Qualitative and quantitative comparison of PET/CT and PET/MR imaging in clinical practice. *J Nucl Med.* 2014;55:88–94.